Development of hybrid (high β) plasmas for D-T operation in JET

C D Challis[1], J Hobirk[2], A Kappatou[2], E Lerche[1,3], F Auriemma[4], E Belonohy[1], F J Casson[1], I Coffey[5], J Eriksson[6], A R Field[1], M Fontana[1,7], J Garcia[8], A Ho[9], F Jaulmes[10], D Keeling[1], D King[1], K Kirov[1], M Lennholm[1,11], C Maggi[1], J Mailloux[1], M Maslov[1], S Menmuir[1], G Pucella[12], E Rachlew[13], F Rimini[1], A Sahlberg[6], A Sips[11], E R Solano[14], C Stuart[1], M Valisa[4] and JET Contributors[*]

[1]*UKAEA, CCFE, Culham Science Centre, Abingdon, Oxon, OX14 3DB, UK*

[2]*Max-Planck-Institut für Plasmaphysik, D-85748 Garching, Germany*

[3]*Laboratory for Plasma Physics LPP-ERM/KMS, B-1000 Brussels, Belgium*

[4]*Consorzio RFX CNR-ISTP, Corso Stati Uniti 4, 35127 Padova, Italy*

[5]*School of Mathematics and Physics, Queen's University, Belfast, BT7 1NN, UK*

[6]*Department of Physics and Astronomy, Uppsala University, SE-75120 Uppsala, Sweden*

[7]*EPFL, Swiss Plasma Center (SPC), CH-1015 Lausanne, Switzerland*

[8]*CEA, IRFM, F-13108 Saint Paul Lez Durance, France*

[9]*FOM Institute DIFFER, Eindhoven, Netherlands*

[10]*IPP of the Czech Academy of Science, Za Slovankou 3, CZ-182 00 Praha 8, Czech Republic*

[11]*European Commission, B-1049 Brussels, Belgium*

[12]*ENEA C. R. Frascati, via E. Fermi 45, 00044 Frascati (Roma), Italy*

[13]*Department of Physics, Chalmers University of Technology, SE-41296 Gothenburg, Sweden*

[14]*Laboratorio Nacional de Fusión, CIEMAT, Madrid, Spain*

After the ITER-like (Be/W) first wall was installed in JET, early experiments showed a restricted operational domain for good confinement quality compared with the previous, predominantly carbon, wall[a]. So, a key aim of the 2021 deuterium-tritium (D-T) campaign was to demonstrate the compatibility of steady high fusion power (10-15 MW) with the ITER-like wall. Plasmas were developed using D fuel, allowing extensive experiments with a high pulse rate and low machine activation. Selected plasmas were repeated and adjusted using T fuel to investigate and mitigate isotope effects. Finally, based on the experience gained with D and T plasmas, D-T experiments were carried out to generate high fusion power with $n_D \approx n_T$.

Compared with 'baseline' plasmas that rely on high plasma current at $q_{95} \approx 3$ to achieve high energy confinement, 'hybrid' scenarios are typically operated at reduced plasma current and increased q_0 (≥ 1) to avoid deleterious MHD modes and access favourable confinement properties at high poloidal β (>1)[b]. This candidate approach for ITER had never previously

[*] *See the author list of J Mailloux et al. 2022 Nucl. Fusion https://doi.org/10.1088/1741-4326/ac47b4*

been tested using T or D-T fuel. The JET 'hybrid' experiments described in this paper were performed at 2.3 MA with a magnetic field strength of ≈3.4 T giving q_{95}≈4.8.

The main phases of the JET 'hybrid' plasma scenario are illustrated in Fig.1. The q-profile at the start of the main heating phase is formed using an Ohmic plasma current 'overshoot'[c]. Analysis of previous mixed H-D JET experiments using low current 'hybrid' plasma scenario showed an increase in central impurity radiation during the Ohmic current ramp phase as the average main ion isotope mass was increased[d]. This led to central plasma cooling, an increase in q_0 and an increased risk of locked modes due to the destabilisation of tearing or double tearing modes at q=2. It was thought to be at least partly due to an expected increase in W sputtering with main ion isotope mass. Predictive modelling suggested that a decrease in core ion temperature as the isotope mass was increased due to decoupling of electrons and ions could also contribute by reducing high Z impurity screening. Both the H-D experiments and predictive modelling indicated that the change in q-profile shape at higher isotope mass could be compensated by increasing the plasma density during the Ohmic current ramp phase. This was confirmed when Ohmic D test pulses were repeated using T plasmas, as shown in Fig.2. An optimised D current ramp was repeated using T fuel, which led to central plasma cooling by radiation. This triggered a real-time 'dud' detector, which aborts the pulse in the case of central cooling to minimise tritium consumption and machine activation in heated pulses with a nonoptimal q-profile. When the T plasma density was increased during the current ramp phase, the q-profile at the typical main heating start time (t≈7 s) was matched to the D reference plasma, as indicated by the matched

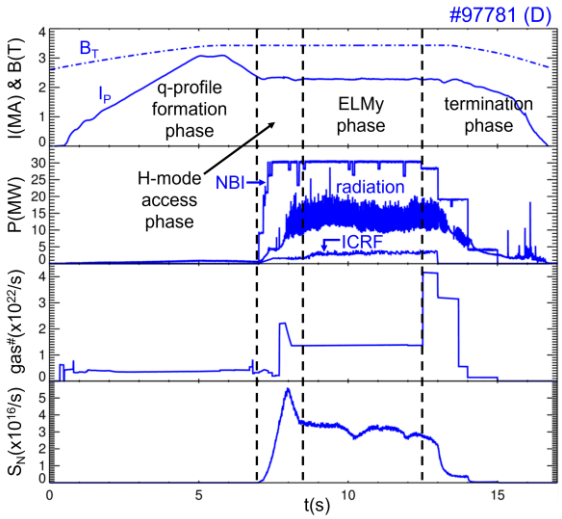

Fig.1. Waveforms for JET 'hybrid' D reference plasma: plasma current & magnetic field, NBI, ICRF & radiated power; requested gas flow (neglecting gas system response time); and neutron rate.

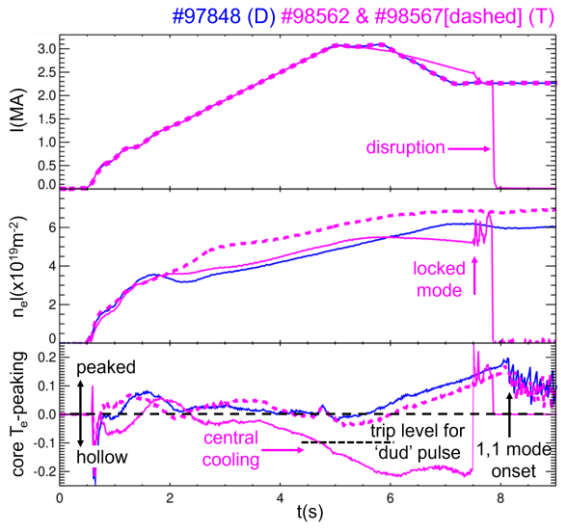

Fig.2. Waveforms for D & T Ohmic test pulses, showing: plasma current; line integrated plasma density; and central electron temperature peaking (=[$T_{e,central}$-$T_{e,off\text{-}axis}$]/$T_{e,off\text{-}axis}$).

onset time of 1,1 MHD modes. This experience enabled the optimum plasma density waveform to be designed for the current ramp phase of the D-T plasmas in advance of the experiments, allowing rapid scenario adaptation.

During the H-mode access phase, indicated in Fig.1, prevention of impurity influxes through the H-mode edge pedestal was the primary method for core radiation control. This was prioritised over the approach of minimising tungsten sources using a detached divertor plasma in order to maximise the H-mode pedestal temperature and access the target range of fusion power for these D-T experiments. A combination of edge temperature screening and ELM flushing was used, which was more challenging for T & D-T plasmas compared with D plasmas as illustrated in Fig.3. High edge ion temperature and low edge radiation was achieved in D reference plasmas by reducing gas injection at the start of the main heating phase to allow a rapid increase in edge ion temperature while delaying the increase in edge density. This is consistent with neoclassical temperature screening of impurities[e]. Then a gas puff was applied during the initial ELM-free phase to trigger a transition to regular type-I ELMs before excessive edge density was achieved. As shown in Fig.3, repeating this with T fuel resulted in an earlier H-mode transition, expected due to the higher main ion isotope mass, and an earlier edge density increase. This was accompanied by a rapid increase in edge radiation, consistent with a loss of impurity screening. Fine adjustment of heating and/or gas fuelling was needed to delay the H-mode transition and avoid excessive edge radiation. Fig.3 shows the optimum waveforms developed to achieve access to an ELMy H-mode with low edge radiation and a hot pedestal in D-T.

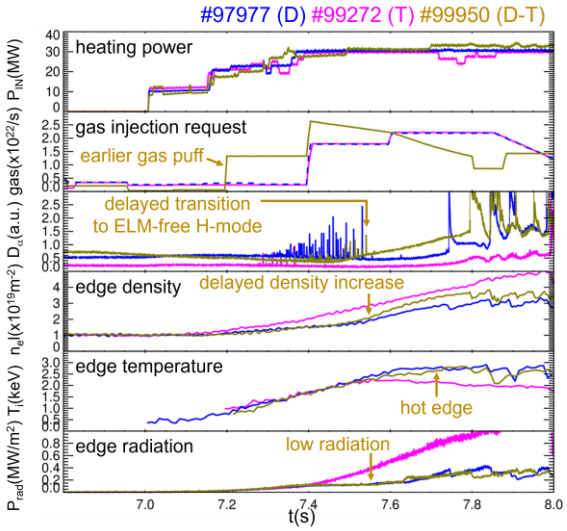

Fig.3. Waveforms for D, T & D-T H-mode access phases, showing: heating power; requested gas flow (neglecting gas system response time); Dα emission; line averaged edge density; edge ion temperature; and edge plasma radiation.

Sustaining low or moderate radiation for several seconds with $H_{98} \geq 1$ required steady high heating power and fine tuning of the gas injection rate. Transient reductions in heating power resulted in reductions in both edge temperature and ELM frequency, which allowed the edge radiation to increase. Insufficient gas injection rate also resulted in a low ELM frequency and a radiation increase, whereas excessive gas injection resulted in a high ELM frequency, low edge temperature and reduced fusion performance. Finding the optimum gas flow rate, balancing these effects, was crucial to the achievement of steady high fusion power.

Even with an optimum plasma edge, central plasma radiation often started to increase after 2-3 seconds, despite the application of 3-4 MW of on-axis ICRF H-minority heating (dominantly to the electrons). The observed central radiation increase did not lead to disruptions during the main heating phase of D-T plasmas but a decrease in fusion power was seen in some cases, as shown in Fig.4. Central impurity radiation has been linked to core MHD modes in this type of plasma[g], which typically appear on this timescale. However, core electron density peaking increases in the early ELMy H-mode phase and also correlates with impurity radiation peaking, qualitatively consistent with predictive modelling, including energy, particle, momentum, current and density channels for main ions and impurities self-consistently[h]. Unlike ITER, JET uses a positive-ion NBI system, which provides strong central fuelling. Simulations with the NBI fuelling artificially turned off showed reduced density peaking and an absence of significant central plasma cooling due to impurity radiation.

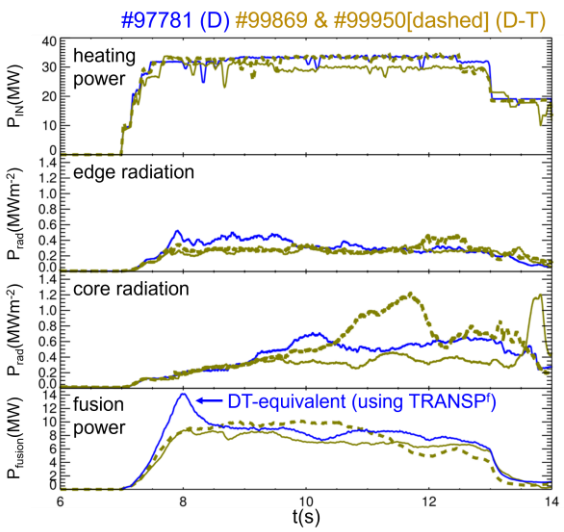

Fig.4. Waveforms for high performance D & D-T plasmas, showing: heating power; edge radiation; radiation from vertical chord through plasma centre; and fusion power.

After careful adaptation of the 'hybrid' plasma scenario for D-T, high fusion power was achieved, broadly consistent with previous modelling predictions[i] given the available heating power. This led to a record fusion energy for a plasma with $n_D \approx n_T$ of ≈46 MJ. Valuable experience was also gained of relevance to ITER relating to: the adaptation of plasma scenarios to different main ion isotopes; the application of edge impurity screening; and the use of modelling to guide scenario development with the aim of achieving high fusion power.

This work has been carried out within the framework of the EUROfusion Consortium, funded by the European Union via the Euratom Research and Training Programme (Grant Agreement No 101052200 — EUROfusion) and from the EPSRC (grant number EP/W006839/1). Views and opinions expressed are however those of the author(s) only and do not necessarily reflect those of the European Union or the European Commission. Neither the European Union nor the European Commission can be held responsible for them.

[a] *E Joffrin et al 2014 Nucl Fusion **54** 013011*
[b] *J Garcia & G Giruzzi 2010 Phys Rev Lett **104** 205003*
[c] *J Hobirk et al 2012 Plasma Phys Control Fusion **54** 095001*
[d] *C D Challis et al 2020 Nucl Fusion **60** 086008*
[e] *S P Hirshman & D J Sigmar 1981 Nucl Fusion **21** 1079*
[f] *R J Goldston et al 1981 J Comput Phys **43** 61*
[g] *T C Hender et al 2016 Nucl Fusion **56** 066002*
[h] *F Casson et al 2020 Nucl Fusion **60** 066029*
[i] *J Garcia et al 2019 Nucl Fusion **59** 086047*